Published in final edited form as:
Biomaterials. 2010 December ; 31(34): 9092–9105. doi:10.1016/j.biomaterials.2010.08.022.

Citric acid-derived *in situ* crosslinkable biodegradable polymers for cell delivery

Dipendra Gyawali[a,b], **Parvathi Nair**[a,b], **Yi Zhang**[a,b], **Richard T. Tran**[a,b], **Chi Zhang**[c], **Mikhail Samchukov**[c], **Marina Makarov**[c], **Harry Kim**[c], and **Jian Yang**[a,b,*]

[a]Department of Bioengineering, The University of Texas at Arlington, Arlington, TX 76019

[b]Joint Biomedical Engineering Program, The University of Texas Southwestern Medical Center and The University of Texas at Arlington, Dallas, TX 75390

[c]Department of Research, Texas Scottish Rite Hospital for Children, Dallas, Texas 75219

Abstract

Herein, we report the first citric acid (CA)-derived *in situ* crosslinkable biodegradable polymer, poly (ethylene glycol) maleate citrate (PEGMC). The synthesis of PEGMC could be carried out via a one-pot polycondensation reaction without using organic solvents or catalysts. PEGMC could be *in-situ* crosslinked into elastomeric PPEGMC hydrogels. The performance of hydrogels in terms of swelling, degradation, and mechanical properties were highly dependent on the molar ratio of monomers, crosslinker concentration, and crosslinking mechanism used in the synthesis process. Cyclic conditioning tests showed that PPEGMC hydrogels could be compressed up to 75% strain without permanent deformation and with negligible hysteresis. Water-soluble PEGMC demonstrated excellent cytocompatibilty *in vitro*. The degradation products of PPEGMC also showed minimal cytotoxicity *in vitro*. Animal studies in rats clearly demonstrated the excellent injectability of PEGMC and degradability of the *in situ*-formed PPEGMC. PPEGMC elicited minimal inflammation in the early stages post-injection and was completely degraded within 30 days in rats. In conclusion, the development of CA-derived injectable biodegradable PEGMC presents numerous opportunities for material innovation and offers excellent candidate materials for *in situ* tissue engineering and drug delivery applications.

Keywords

biodegradable elastomers; *in situ* crosslinking; cell encapsulation; drug delivery; tissue engineering

1. Introduction

Seeking ideal biomaterials for specific biomedical applications has been an ongoing effort in biomedical engineering. Carefully selecting monomers for biomaterial syntheses is essential for determining and controlling the functionality and biocompatibility of the biomaterials to be produced. Citric acid (CA) is a multifunctional chemical compound that is involved in Kreb cycle and used in many aspects of our lives such as in food additives, water softening, anti-

*Corresponding author. Tel.: 817-272-0562; fax: 817-272-2251. jianyang@uta.edu (J. Yang).

coagulant, anti-viral tissues, and cleaning products. In recent years, there has been increasing attention in using citric acid as a robust multifunctional monomer for biomaterial syntheses. A key feature for CA-derived biomaterials is that CA provides valuable pendant functionality participating in the ester bond-crosslink formation, enhancing hemocompatibility, balancing the hydrophilicity of the polymer network, and providing hydrogen bonding and additional binding sites for bioconjugation to confer additional functionality such as optical properties. [1,2]

The recent developments on citric acid-derived biomaterials were driven by the significant needs for biodegradable elastomers in tissue engineering. Poly(diol citrate) was the first type of CA-derived biodegradable elastomer.[3,4] CA reacted with aliphatic diols such as 1,8-octanediol to form oligomers (prepolymers) which can be crosslinked into elastomeric polyesters, poly (diol citrates). Poly(diol citrates) have shown promise as biomaterials for hemocompatible and compliant vascular graft coatings,[5] small diameter blood vessel and cartilage tissue engineering,[6] and orthopedic fixation devices.[7] More recently, significant efforts in our laboratories have focused on expanding the tunability and functionality of the citric acid-derived biodegradable elastomers. By doping urethane bonds in a polyester network, crosslinked urethane-doped polyester (CUPE) was developed based on poly(diol citrate). CUPE addresses the challenges in developing soft, elastic but strong biodegradable elastomers that can serve as immediately implantable tissue engineering scaffolding materials for *in vivo* tissue engineering.[2,8] By introducing double-bond-containing monomers into the poly (diol citrates) prepolymer network, such as maleic acid and maleic anhydride, poly(alkylene maleate citrates) (PAMCs) were synthesized.[9,10] PAMCs feature a dual-crosslinking mechanism through which the polymers can be crosslinked by ester-bond formation as similar to poly(diol citrates) and photocrosslinking polymerization due to the presence of double bonds from the maleate units in the polymer backbones. This dual-crosslinking mechanism allows fine tuning the mechanical properties and degradation rates of PAMCs to better fit the versatile needs in various soft tissue engineering. Even more exciting development made recently, the first biodegradable photoluminescent polymers (BPLPs) were developed by adding α-amino acids to poly(diol citrates) polymer backbones.[11] The side-added amino acids further reacted with the germinal –OH on the same citrate units to form fluorescent 6-membered amide-ester rings which resulted in bright fluorescence with high quantum yields (up to 79%) and tunable fluorescence emission (up to 825 nm). The fully degradable photoluminescent polymers hold great promise for tissue engineering and drug delivery where quantitatively non-invasive or minimally-invasive monitoring or tracking of scaffold degradation/tissue regeneration and drug delivery processes remain challenges.

In recent years, *in situ* crosslinkable biodegradable materials have gained much attention for potential applications in tissue engineering, drug delivery, and wound care.[12–18] For tissue engineering applications, *in situ* crosslinkable biodegradable materials can be used as injectable scaffolds for tissue regeneration through a minimally-invasive delivery method. [19,20] For drug delivery applications, injectable biomaterials can be used for the localized delivery of therapeutic agents to a diseased site avoiding dangerous and costly surgical procedures.[21] A wide variety of *in situ* crosslinkable biomaterials have been reported ranging from naturally derived extracellular matrices (ECM) such as chemically-modified glycosaminoglycans (GAGs)[22–27] to synthetic polymers such as poly (vinyl alcohol) (PVA)[28,29], poly (ethylene glycol) (PEG) [30,31], poly(propylene fumarate) (PPF) [32,33], polyphosphoester [34,35], and polylactone-based hydrogels[36–38].

Given the aforementioned benefits of using citric acid for biomaterial syntheses and the fact that none of the previously developed citric acid-derived biodegradable elastomers can be made into a water soluble form for *in situ* drug and cell delivery, herein, we reported the syntheses and characterization of the first citric-acid derived water-soluble, *in situ* crosslinkable, and

biodegradable polymers, poly(ethylene glycol) maleate citrates (PEGMCs). PEGMCs were synthesized by reacting citric acid (CA) with poly (ethylene glycol) (PEG) 200 and maleic acid (MA). PEGMCs can be *in-situ* crosslinked into biodegradable elastomeric polyester hydrogels (PPEGMCs). CA is a multifunctional acid and a metabolic product of the Krebs cycle.[39] PEG is the most widely used water-soluble macro diol in biomedical applications. MA, an important component of the citric acid cycle, has been used in many synthetic biomaterial designs, and was chosen as a difunctional acid bringing vinyl functionality to the polymers.[40–43]

2. Materials and Methods

All chemicals, cell culture medium, and supplements were purchased from Sigma-Aldrich (St. Louis, MO), except where mentioned otherwise. All chemicals were used as received.

2.1. Synthesis and characterization of PEGMC

PEGMC is an oligomer (prepolymer) which was synthesized as described in Fig. 1. CA, PEG, and MA were melted in a 250 ml three-necked round bottom flask fitted with an inlet adapter and outlet adapter by stirring the contents in the flask at a temperature of 160 °C under nitrogen gas flow for 20 minutes. Once the constituents melted, the temperature was reduced to 145 °C for 2 hours. The pressure was then dropped to 50 mTorr for another 2 hours. The prepared prepolymer was dissolved in deionized water and dialyzed with a 500 Dalton molecular weight cut off membrane for 2 days followed by lyophilization to achieve a purified form of PEGMC (pre-PPEGMC). Different ratios of acids (MA/CA) were adjusted in the initial composition of the prepolymer as 8/2, 6/4, and 4/6, respectively, as shown in Table 1. The overall ratio of the acids over the diol was kept at 1:1.

To analyze the functional groups present in PEGMC, a 5% (w/v) PEGMC solution in 1,4-dioxane was prepared and cast onto a potassium bromide crystal and allowed to dry overnight in a vacuum hood. Fourier Transform Infra Red (FT-IR) spectroscopy measurements were recorded at room temperature using a Nicolet 6700 FT-IR (Thermo Scientific, Waltham, MA) equipped with OMNIC Software using 128 scans across the wave numbers 4000 − 400 cm^{-1} at a resolution of 2 cm^{-1}. For proton analysis, the prepolymers were purified twice as mentioned above and then dissolved in dimethyl sulfoxide-d6 (DMSO-d6) to make a 3% (w/v) prepolymer solution and placed in a 5 mm-outer diameter tube. Proton Nuclear Magnetic Resonance (^{1}H-NMR) was used for the analysis of the actual composition of PEGMCs for all ratios on 300 MHz JNM ECS 300 (JEOL, Tokyo, Japan). The chemical shifts for the ^{1}H-NMR spectra were recorded in parts per million (ppm), and were referenced relative to tetramethylsilane (TMS, 0.00 ppm) as the internal reference.

2.2. Preparation and Characterization of PPEGMC Hydrogel

For the crosslinking of PPEGMC by photo-initiators, the purified pre-polymer was dissolved in water to make a 30% polymer by weight concentration. Acrylic acid was used as a crosslinker and 2,2'-Azobis(2-methyl propionamidine) dihydrochloride was used as a photoinitiator. In this study, the percentage of photoinitiator was fixed as 0.11 M, whereas the concentration of crosslinker was varied as 1.5–6% (w/v) to study the effect of crosslinker on the overall hydrogel performance. Next, the solution was poured into a Teflon mold and placed under a UVP 365 nm Long Wave Ultraviolet Lamp (Upland, CA) for 60 seconds.

For the crosslinking of PPEGMC by water-soluble redox initiators, a 30% (w/v) pre-polymer solution in water was mixed with 3% (w/v) of acrylic acid. The mixture was then added to an aqueous solution of 0.026 M ammonium persulfate (APS) and 0.11 M *N*,*N*,*N*′,*N*′-tetramethylethylenediamine (TEMED). Next, the mixture was placed in an air tight vial and

incubated at 37° C for 60 seconds. The schematics of polymer syntheses are shown in Fig. 1. The resulting PPEGMC was characterized by FTIR to verify the crosslinking formation as compared to the PEGMC.

2.3. Sol content of PPEGMC Hydrogel

Sol content was determined by measuring dry mass differential before and after incubation with 1,4-dioxane, which dissolves unreacted prepolymers. Freshly made photocrosslinked hydrogels were lyophilized for 48 hours to achieve dry hydrogel discs and weighed (M_i). These hydrogel discs were immersed in 1,4-dioxane for 2 days and further lyophilized and weighed (M_f). The sol gel fraction (SFG%) was calculated using Equation 1. Sol content experiments were also designed to understand the effect of MA/CA ratio in the polymer chain, amount of crosslinker, and crosslinking mechanism (photo and redox) on the sol content of the hydrogel.

$$\text{sol}\,(\%) = \frac{M_i - M_f}{M_i} \times 100 \tag{1}$$

2.4. Swelling ratio of PPEGMC Hydrogel

Sol free lyophilized PPEGMC discs were incubated in PBS, deionized water, and buffer solutions with different pHs (2.4, 3.4, 4.4, 5.4, 6.4, 8.4, 9.4, 10.4) until the equilibrium state was achieved (2 days). The surface of the swollen discs was gently blotted with filter paper to remove any excess swelling agent. The samples were then weighed (M_w). The discs were again lyophilized for 3 days and weighed to determine the dry weight (M_d). Equation 2 calculated the equilibrium-swelling ratio. The effect of different ratios of MA/CA and crosslinking mechanism on the swelling ability of PPEGMC hydrogel was also evaluated in this study.

$$\text{swelling}\,(\%) = \frac{M_w - M_d}{M_d} \times 100 \tag{2}$$

2.5. Mechanical Properties of PPEGMC

The tensile mechanical properties were studied according to the ASTM D412a standard on a MTS Insight II mechanical tester equipped with a 500 N load cell (MTS, Eden Prairie, MN). Photo-crosslinked and lyophilized PPEGMC films were cut using a dog bone shaped (26 mm × 4 mm × 1.5 mm, length × width × thickness) aluminum die. The dog bone shaped films were pulled until failure at a rate of 500 mm/min to obtain the stress strain curves. The initial slope (0–10%) of the curve was used to determine the initial modulus of the material.

Compressive tests were performed in an unconfined state using MTS Insight II mechanical tester with a 10 N load cell. Tests were performed on the freshly prepared redox-crosslinked cylindrical hydrogels with dimensions of 10 mm in thickness and 10 mm in diameter. Compression (%) and load (N) were recorded using Testworks 4 software at a cross-head speed of 1 mm/min at various strain levels. The samples were cyclically preconditioned for 30% strain for the first cycle. The hydrogels were subsequently subjected to another loading and unloading cycle with increments of 10% strain level until the failure. The compressive modulus (0–10%) of the final cycle was obtained as the tangent slope of the stress-strain curve.

2.6. *In Vitro* tests

In order to evaluate the in vitro degradation of PPEGMC hydrogel, sol free lyophilized PPEGMC discs were weighed to find the initial mass (M_o), suspended in PBS (pH 7.4), and maintained at 37 °C. The pH was monitored, and the buffer was replaced every day for first week and thereafter once a week to ensure a constant pH of 7.4. At the desired time point, the

samples were rinsed with deionized water, lyophilized, and weighed to find the remaining mass (M_t). The sample morphology changes over degradation times were recorded by a Hitachi S-3000N scanning electron microscope (Hitachi, Pleasanton, CA). The percent mass loss (% ML) was calculated by Equation 3.

$$\text{mass loss}\ (\%) = \frac{M_0 - M_t}{M_0} \times 100 \tag{3}$$

Bovine serum albumin (BSA, *M*W = 67000 g/mol) was chosen as the model protein for the protein release study. A BSA solution was first prepared by dissolving 2.0 g of BSA in 40 mL of PBS solution (pH 7.4). Then, the appropriate amount of the BSA solution was mixed with the polymer solution to make a 1:20 protein to polymer weight ratio. This mixture was photocrosslinked with 0.11 M of PI and 3 v/v% of acrylic acid for 1 min. The resulting BSA-loaded PPEGMC hydrogels were lyophilized for 48 hr. The *in vitro* release was carried out in glass tubes at 37°C in a PBS buffer solution (pH 7.4) and a sodium acetate-acetic acid buffer solution (pH 5.4). At each predetermined time, BSA-released buffer solution was removed from the glass tube and fresh buffer solution was added into the glass tubes. The cumulative release of BSA was quantified by a UV Spectrophotometer (Lambda Bio40 UV–*vis* spectrometer, Perkin-Elmer) at 280 nm.

PEGMC solutions were prepared in deionized water buffered with excess sodium bicarbonate until the pH was maintained at 7 to perform *in vitro* cytotoxicity evaluation. The solution was lyophilized and diluted with Dulbecco's modified eagle's medium (DMEM) supplemented with 10% (v/v) fetal bovine serum, 100 U/ml penicillin, and 100 μg/ml streptomycin at various concentrations (1, 0.1, 0.01) g/100 ml and sterilized through 0.2 μm filter. 200 μL of 3T3 mouse fibroblasts in DMEM (5×10^4 cells/mL) was added to each well in a 96-well plate and then incubated for 24 h at 37° C, 5% CO_2. The culture medium was changed to 200 μL of DMEM containing the prepolymers with particular concentration and was incubated for another 12 h. A methylthiazoletetrazolium (MTT) cell proliferation and viability assay was used for a quantitative assessment of the viable cells according to the manufacturer's protocol. Viability of cells in the presence of PPEGMC pre-polymers was compared to the ones with poly (ethyleneglycol)diacrylate (PEGDA 3.5 kDa) pre-polymer and normalized to the viable cells cultured with medium without polymers.

For the evaluation of cellular response on the surface of the hydrogel, photo-crosslinked hydrogels were transferred into a 48-well plate and washed with ethanol, followed by an exposure to UV radiation for 30 min to for sterilization. The hydrogels were then equilibrated in a complete DMEM culture media at 37 °C overnight. Both NIH 3T3 fibroblasts and human dermal fibroblasts were then seeded on the hydrogels at 1×10^5 cells/well. Cells were cultured in a CO_2 incubator for 48 h at 37 °C, and the morphology of the adhered cells were analyzed using an inverted microscope (Zeiss Auxiovert).

Water-soluble redox initiators were used for cell encapsulation in crosslinked PPEGMC hydrogel. 0.3 g of PPEGMC pre-polymer was first dissolved in 400 μL of deionized-H_2O and mixed with 3% (v/v) of (Acrylic Acid) crosslinker to the final volume of the solution. Then, the mixture was buffered with sodium bicarbonate until the pH was maintained at 7. The mixture was then added to the initiator solutions, 0.026 M ammonium persulfate (APS) and 0.11 M *N*,*N*,*N*′,*N*′-tetramethylethylenediamine (TEMED) in water. Next, the mixture was quickly sterilized through a 0.2 μm filter and added to a cell suspension of 10 million cells in 270 μl of PBS to achieve a final suspension concentration of 10 million cells/ml. Immediately after mixing, the suspension was injected into an air sealed mold and maintained at 37 °C incubator for 5 min. Live and dead cells in the gel were stained with LIVE/DEAD Viability/

Cytotoxicity Kit, (Invitrogen) according to manufacture protocol after 48 h of incubation under a humidified atmosphere at 37 °C with 5% CO_2. To observe the morphology of the encapsulated cells, cells were pre-stained with carboxyfluorescein diacetate-succinimidyl ester (CFDA-SE) green fluorescent cell tracer using the manufacturer's protocol.

For testing the cytotoxicity of PPEGMC degradation products, PPEGMC hydrogels with all three different monomer ratios were allowed to degrade in 0.2 M of NaOH. The pH of the solution was adjusted to pH 7.4 with 0.2 M of HCl. The polymer degradation solutions were diluted with DMEM into various concentrations. 200 μL of 3T3 mouse fibroblasts in DMEM (5×10^4 cells/ml) was added in a 96-well plate and incubated for 24 h at 37° C, 5% CO_2. The culture medium was then replaced by 200 μL of DMEM containing the degraded hydrogel product with various concentrations and was incubated for another 12 h. A methylthiazoletetrazolium (MTT) cell proliferation and viability assay was used for a quantitative assessment of the viable cells according to the manufacturer's protocol. poly(L-lactide) (PLLA, 99 kDa, Sigma) was used as a control. Viability of cells in the presence of PPEGMC degradation products was normalized to the viable cells cultured with regular complete DMEM medium.

2.7. Foreign Body response to PPEGMC hydrogel

To demonstrate the *in situ* formation of gels *in vivo* and to understand the host response to the crosslinked gels, sterile hydrogel precursor solutions as described in section 2.6 were prepared. 250 μL of the solution was injected subcutaneously with a 27-gauge needle into 7-week-old female Sprague-Dawley rats (Harlan Sprague Dawley, Inc., Indianapolis, IN) under deep isoflurane-O_2 general anesthesia. Animals were cared for in compliance with the regulations of the Animal Care and Use Committee of The University of Texas at Arlington. PPEGMC samples were injected symmetrically on the upper and lower back of the same animal. All the animals were observed daily for any change in their behavior over the period of experiment. At each pre-determined time point (5, 15, and 30 d), three animals were sacrificed with excess CO_2, and polymers with surrounding tissues were harvested for further evaluation. The explants were fixed by soaking in 10% formalin for 2 days. The samples were processed on an automated tissue processor, embedded in paraffin wax, and sectioned into 5-μm sections. Six slides from different areas of the explants were stained with hematoxylin and eosin staining. Additionally, six slides were immunostained with for CD68 (a glycoprotein expressed on monocytes/macrophages) using rabbit anti-rat CD68 primary antibody (1:200, Abcam, England, UK) followed by goat anti-mouse secondary antibody (Vector Burlingame, CA, USA) to identify macrophage recruitment. Samples were incubated with strepavidin horseradish peroxidase (1:100, Dako, Denmark) and developed with DAB substrate chromogen (Dako). The cross-sections were examined using a Leica DMLP microscope (Leica Microsystems Inc., Bannockburn, IL) fitted with a Nikon E500 camera (Nikon Corp., Japan)

2.8. Statistical Methods

All the experiments of sol gel content, swelling ratio, mechanical test, degradation profile, and MTT assays were performed in six samples (n=6). MTT metabolism assays were performed with triplicate readings for each data point. Histological macrophage scoring was also based on at least 10 randomly selected images. Data are expressed as mean ± standard deviation. Statistical analysis was performed using one way-ANOVA with post hoc Neuman–Keuls testing. A p-value of 0.01 or less was considered statistically significant.

3. Results

3.1. Syntheses and characterization of PEGMC

The syntheses of PEGMCs were convenient. The simple one-pot polycondensation reaction between macro diol (PEG200) and acids (MA and CA) did not require any organic solvent or toxic catalyst. A transparent viscous PEGMC was achieved within 4–6 h of reaction time. PEGMCs consist of degradable ester bonds (C=O at 1690–1750 cm^{-1} and C-O at 1000–1260 cm^{-1}), pendant carboxylic and hydroxyl groups (C=O at 1690–1750 cm^{-1} and-OH at 3570 cm^{-1}), and double bonds (C=C at 1650 cm^{-1}) as confirmed by FTIR spectra (Fig. 2 A). The random copolymers exhibited characteristic peaks of MA (a, a'), CA (b), and PEG (c, d) in a representative ^{1}H-NMR spectra of PEGMC 8/2 (Fig. 2 B). The polymer compositions characterized by ^{1}H-NMR matched the monomer feeding ratios as shown in Table 1. In the case of PEGMC 8/2, all the multiple peaks of vinyl hydrogen were intensified, however when the amount of MA was reduced as in the case of PEGMC6/4 and PEGMC4/6, peaks towards lower chemical shift (peaks a) significantly diminished. This data suggested that in all cases, PEGMC polymer chains are terminated with maleate moieties (peaks a'). However, in case of higher MA/CA molar ratio polymer chains (PEGMC8/2 and PEGMC 6/4), significant amounts of maleates were also incorporated within the chains (peak a) except on the chain ends. These results indicated the successful syntheses of PEGMCs with controlled polymer compositions.

3.2. Preparations and Characterization of PPEGMC Hydrogel

PEGMCs can be crosslinked via free radical initiators (photo and redox) within 60 seconds. PPEGMC hydrogels are translucent in nature. Crosslinking of the hydrogel was achieved by the consumption of the vinyl moiety contributed via MA whereas pendant carboxylic and hydroxyl functionalities were still preserved as indicated by FTIR in Fig. 2 A. Crosslinking of PEGMC was aided with the use of terminal alkene crosslinker (in this case, acrylic acid).

3.3. Sol content of PPEGMC hydrogel

Fig. 3 showed the dependence of sol content of PPEGMC on the molar ratio of acids, the concentration of crosslinker, and the mode of crosslinking mechanism. The results indicated that there was no significant difference in sol content when the concentration of MA was higher than CA as in case of PPEGMC 8/2 (29.6± 2.9 %) and PPEGMC 6/4 (29.0± 3.3 %), but it significantly dropped when the concentration of CA exceed MA in the pre-polymer chains as in the case of PPEGMC 4/6 (20.7±1.7 %) (Fig. 3 A). On the other hand, if the amount of crosslinkers increased in the hydrogel precursor solution, the sol content significantly decreased. For example, sol content decreased significantly from 45.0±1.0% to 15.0±14.9 % as crosslinker concentration increased from 1.5% to 6.0% (v/v) ($p < 0.01$) (Fig. 3 B). It was also observed that the crosslinking mechanism had a significant effect on the sol content of PPEGMC. There was about 2-fold decrease in sol content if the hydrogel was crosslinked with redox initiators (14.6±1.5) as compared to photocrosslinked hydrogel (29.0±3.3) (Fig. 3 C). This could be explained with the fact that a homogeneous crosslinking might not be achieved in photo-crosslinking due to the uneven light illumination throughout the solution.

3.4. Swelling ratios of PPEGMC hydrogel

The swelling of the PPEGMC hydrogels were investigated by incubating the polymers in PBS, water, and buffers with different pH at 37° C for 48 hours. Fig. 4 showed the effect of monomer molar ratio (MA/CA), crosslinking modes, and pH of swelling medium on swelling degree of PPEGMC hydrogels. The results showed that the swelling increased in both PBS (6.9±0.3 to 15.2±1.2) and H_2O (1.0±0.2 to 2.5±0.2) when monomer ratio of MA to CA decreased (Fig. 4A). However, the swelling ratios were higher in all the cases for PBS than those in water. This clearly demonstrates that PPEGMCs were saturated with ionizable functionalities (i.e., COOH

groups). In addition to this, swelling ratio of PPEGMC was significantly reduced in the hydrogel PPEGMC 6/4 crosslinked by redox initiators in both PBS and water as compared to that of photocrosslinked PPEGMC 6/4 (Fig. 4 B). For a more in depth understanding of the ionizable functionalities presented in these hydrogels, we performed another swelling study on buffers with various pH levels. Fig. 4 C indicated that all the hydrogels restricted their swelling ability when pH was lower than 5.4. There was a significant increase in the swelling ability of all hydrogels in the pH levels between 5.4 and 7.4. Furthermore, this gradient in the swelling was more significant on the hydrogel with higher CA content.

3.5. Mechanical properties of PPEGMC hydrogel

The stress-strain curves of photo-crosslinked PPEGMC shown in Fig. 5 A are characteristic of elastomers. PPEGMC with a higher molar ratio of CA exhibited higher ultimate tensile strength at break and higher elongation. PPEGMC 8/2 possessed 138.0% of elongation and 311.0 KPa of tensile strength while PPEGMC 4/6 possessed 638.0 KPa of tensile strength and 723% of elongation at break. However, the initial modulus of PPEGMC8/2 (777.2 ± 109.4 KPa) was significantly higher than that of both PPEGMC6/4 (450.0 ± 25.6KPa) and PPEGMC4/6 (388.7± 54.8 KPa) (Fig. 5 B).

Redox-initiated crosslinked PPEGMC hydrogels were compressed to 70% strain under cyclic compression, and it was found that the materials did not undergo any permanent deformation. Under cyclic compression, very minimal hysteresis was observed for all three types of hydrogels as compared to other reported hydrogels [44], demonstrating their excellent elastic properties. PPEGMC6/4 held highest ultimate compressive strength (231.0 KPa) before failure at a compressive strain of 79.0% compared to PPEGMC8/2 (compressive strength of 69.0 KPa at 64.0% of strain) and PPEGMC4/6 (compressive strength of 101.0 KPa at 79.0% of strain) (Fig. 5 C). However, the compression modulus of PPEGMC8/2 (18.0 ± 1.5 KPa) was significantly higher than both PPEGMC6/4 (11.0 ± 1.2 KPa) and PPEGMC4/6 (8.0 ± 1.5 KPa) (Fig. 5 D).

3.6. *In vitro* tests

Fig. 6 showed the kinetics of PPEGMC hydrogel mass loss and surface morphology changes of the hydrogel upon degradation. Photo-crosslinked PPEGMC4/6 was completely degraded within 30 d time period whereas PPEGMC8/2 lost 73.3 ± 2.6% of its initial mass. When compared to redox initiator crosslinked PPEGMC6/4 which lost 70.1 ± 2.03% of its mass, photocrosslinked PPEGMC6/4 already lost 95.4 ± 1.9% of its initial mass within 30 d (Fig. 6 A). It was also observed that the amount of crosslinker used for crosslinking also influenced the degradability of the hydrogels (Fig. 6 B). PPEGMC hydrogels prepared with 6% of crosslinker degraded 78.5 ± 2.0% of its mass compared to hydrogels prepared with 1.5% of crosslinker which degraded completely within 30 d. It was observed that as the degradation proceeded, the hydrogels became more porous (Fig. 6 C–E). This might be an important property of PPEGMCs as scaffolding materials for tissue engineering, where cell infiltration to the matrix is very critical as the matrix degrades.

In Vitro release of BSA from PPEGMC hydrogels was observed over a 5-day period in PBS buffer (pH = 7.4) and sodium acetate-acetic acid buffer (pH 5.4). After initial burst release, the BSA release rate was in the sequence of PPEGMC 4/6 (92.7 ± 2.0%) > PPEGMC 6/4 (85.2 ± 3.8%)> PPEGMC 8/2 (73.1 ± 1.8%) over 5 d period at pH 7.4 (Fig. 7 A). However, the release rate was in the sequence of PPEGMC 8/2 (61.8 ± 2.9%) > PPEGMC 6/4 (32.1 ± 3.5%)> PPEGMC 4/6 (28.2 ± 1.4%) when incubated at pH 5.4 (Fig. 7 B).

Fig. 8 shows that the PPEGMC hydrogel provided a good substrate for cells when seeded on the surface or embedded within the *in situ* forming hydrogel. Both cell types, NIH-3T3s (Fig.

8 A) and human dermal fibroblasts (Fig. 8 B), adhered and spread upon the hydrogel surfaces within 48 h. When encapsulated in the network of the PPEGMC hydrogels, more than 80% of NIH-3T3s were stained alive (Fig. 8 C). These cells began to spread within the networks of PPEGMC 48 h after encapsulation and gel formation (Fig. 8 D).

The cytotoxicity of PPEGMC prepolymer (PEGMC) and the degradation products of PPEGMC were also evaluated. We evaluated the viability of NIH 3T3 cells in the presence of PPEGMC prepolymers compared to the prepolymer of PEGDA (Fig. 9 A) and degradation products of PPEGMC compared to degraded product of PLLA (Fig. 9 B) at various concentration. Upon 12 h of incubation of cells, there was no difference on cell viability for both PEGMC and PEGDA prepolymers (3.5 kDa). However, there was a slight increase in the level of cell viability as the concentration of PEGMC decreased. Similarly, cells cultured with the degradation products of PPEGMC hydrogels also showed similar viability to the cells cultured with the degradation products of PLLA under similar concentrations.

3.7. *In situ* crosslinkability and foreign body response to PPEGMC

To demonstrate the injectability of PPEGMC, PEGMC aqueous solution was injected into a rat animal model for *in situ* forming of PPEGMC hydrogels. Water-soluble redox initiator was used to mix with PEGMC solution and then subcutaneously injected into rats through a 27-gauge needle. PEGMC quickly formed gel *in situ* a few minutes after injection (Fig. 10A). It was later (after 30 d) confirmed that the crosslinked hydrogels were completely absorbed by the host without any noticeable changes to the surrounding tissues (Fig. 10B).

Over the course of experiment, test animals did not show any abnormalities in their physical and behavioral patterns such as weight loss, lethargy, anorexia, and dehydration, nor did they exhibit signs of distress. Histology analysis showed a presence of inflammatory cells at both 5 d and 15 d implantation (Fig. 11). However, the number of cells around implants was significantly decreased at day 30 (Fig. 11). The CD68 positive cells (monocytes/macrophages) around the implants (Fig. 11) were counted and normalized to the total stained tissue area to determine the extent of inflammation. The number of CD68 positive cells did not significantly increase with increasing implant duration from day 5 to day 15 (Fig. 12). However, the number of macrophages was significantly decreased as the material was completely absorbed by the host at 30 d (Fig. 11 and Fig. 12).

4. Discussion

The development and applications of citric acid-derived biodegradable polymers has attracted much attention in recent years. All these polymers share an important key monomer, citric acid, in synthesis. However, none of the previous citric acid-derived biodegradable polymers could be used as *in situ* cell/drug carriers for tissue engineering and drug delivery. Previously, we have developed citric acid-derived photocrosslinked elastomers with elastic mechanical properties and rich functional groups by introducing vinyl functionalities to the polymers. However, their poor solubility in water limits their application in various injectable biomedical applications. In this study, we reported a new injectable citric acid-derived *in situ* crosslinkable biodegradable polymer, PPEGMC.

The potential use of injectable biomaterials often depends upon the crosslinking mechanism. For example, a redox-initiating system is preferred in areas of limited light penetration and where homogeneous crosslinking is required, whereas, a photo-initiating system is preferred where temporal and spatial control over the system is required. In addition, the crosslinking mechanism may also play a prominent role on the overall property of the material. In this work, we have studied the effect of crosslinking mechanism (redox and photo) and additional crosslinker on the material properties. The PPEGMC hydrogel exhibited lower swelling

properties, reduced sol content, and slower degradation rates when crosslinked with redox mechanism. The amount of crosslinkers also had a significant impact on the reduction of sol content and degradation rate of the hydrogel. Another important parameter is crosslinking time. Long crosslinking times may not be feasible for practical uses of the injectable materials whereas too rapid crosslinking might hinder the process of implantation. It was realized that the mechanism of crosslinking, the amount of initiator system, and the concentration of crosslinker play significant roles in determining the crosslinking time. In our experiments, all these parameters were carefully chosen to optimize the time window for handling and crosslinking of the polymers without compromising their biocompatibility. As a result, PPEGMC hydrogel precursor could be easily injected and rapidly crosslinked within the targeted site.

Most of the existing hydrogels lack free functional group(s) that are important for potential biofunctionalization. Various attempts have been made in recent years to develop polyester based on multi functional citric acid and maleic acid with a purpose of preserving some of their carboxylic acid and hydroxyl groups. However, the ability to utilize these functionalities for further modification with bioactive molecules is limited as these functional groups were sacrificed in the process of crosslinking.[45] We demonstrated the successful preservation of these carboxylic and hydroxyl groups in the PEGMC polymer chains determined by FTIR and NMR (Fig. 2 A and B) and in the bulk of the crosslinked hydrogel determined by FTIR and swelling study. As seen in the swelling study (Fig. 4), there was a sudden increase in the swelling ability of PPEGMC hydrogels in the buffer of pH 5.4 to 7.4. The difference in the swelling of hydrogels at pH 5.4 to 7.4 revealed that PPEGMC chains contained ionizable groups with their pka values somewhere between 6 and 7. It was believed that these groups are the second carboxylic group of maleic acid ($pk_2 = 6.27$) and the third carboxylic group of citric acid ($pk_3 = 6.4$). Carboxylic and hydroxyl groups were recognized as the highly favored pendant chemistries for functionalization of biomaterials with drugs or biomolecules. The availability of such groups on the PEGMC polymer chains provides sites for potential biofunctionalization.

Another important parameter to be considered for injectable hydrogels is the sol content of the material following crosslinking. As shown in Fig. 3, higher crosslinker concentration and redox crosslinking mechanism produced hydrogels with lower sol content (<15%). However, with higher molar ratios of maleic acid (vinyl containing monomer), there is a higher sol content. This was contradictory to the conventional explanation that as the amount of double bond increased, the sol content would decrease. However, it should be noted that trans conformations of maleic acid would encourage more coiled pre-polymer chains when higher number of maleate units were incorporated in the middle of chains, as confirmed by ^{1}H-NMR study. When these chains were crosslinked via terminal vinyl containing crosslinker in an aqueous solution, intramolecular crosslinking could occur in additional to intermolecular crosslinking. These intra-crosslinked chains could be leached out from the system by the solvent.

Tensile properties of photocrosslinked PPEGMC showed that an increase in molar concentration of citric acid (relatively less maleic acid) resulted in an increase in elongation and ultimate tensile strength and a decrease in initial modulus (Fig. 5 A and B). These data clearly suggested that the presence of citric acid had a significant effect on the mechanical properties of the resulting crosslinked polymers. It was believed that reducing the amount of maleic acid would result in less crosslinking sites (double bonds) for crosslinking, thus reducing crosslinking degree. The reduced crosslinking degree should contribute to longer polymer chains between crosslinks resulting in decreased initial modulus and increased elongation. The increased tensile strength was ascribed to the increased hydrogen bonds among polymer networks due to the increased amount of citric acid. Cyclic compression conditioning tests conducted on water-soluble redox-initiator crosslinked PPEGMCs demonstrated that these

hydrogels were highly elastic and showed 100% recovery with negligible hysteresis (Fig. 5 C). PPEGMC hydrogels were soft as confirmed by the low initial modulus (100–500 kPa) (Fig. 5 D) at dry state in tensile test and 8–28 kPa at wet state in compression tests).

For tissue engineering applications, it would be ideal if the scaffolding material could be degraded gradually into the porous matrix in the process of degradation to facilitate the ingrowths of regenerating tissue. It was expected that PPEGMC should undergo hydrolysis degradation as the polymer chains between crosslinks are polyesters. The degradation studies indicated that PPEGMC hydrogels degraded into porous matrix during the course of degradation (Fig. 6). Results also revealed that as the vinyl moiety in the hydrogel precursor was increased (either increased in MA concentration or crosslinker concentration), the rate of degradation reduced. Redox crosslinked gels showed a further decrease in degradation rates compared to that of photocrosslinked hydrogels. These data conclude that higher crosslinking due to increased concentration of double bonds and homogeneous crosslinking during redox crosslinking resulted in a reduction of degradation rate. It was also observed that redox crosslinked hydrogels were only degraded 70% of their mass in PBS.

The *in vitro* BSA release study showed about 40% initial burst release and then more sustained release over 5-day period from PPEGMC hydrogels in buffer solutions at both pH 7.4 and 5.4. The BSA release studies confirmed the pH sensitivity of PPEGMC networks. The more restricted BSA release from PPEGMC hydrogels at pH 5.4 was ascribed to the acid form of carboxyl groups from citrate units which contributed to the hydrogen bonding with the encapsulated BSA. The higher the citrate content, the slower the BSA release (Fig. 7 A and B). The BSA release study supported that the water-soluble PEGMC can potentially be a viable candidate material for controlled *in situ* protein/drug delivery applications.

One major potential application for PEGMC is to use PPEGMC as an *in situ* forming cell delivery carrier. It is important that the water-soluble PEGMC should have excellent cell compatibility for in-situ crosslinking applications. PEGMC demonstrated minimal cytotoxicity as similar to the commercially available injectable polymer (PEGDA) (Fig. 8 and Fig. 9 A). The degradation products of the crosslinked PEGMC (PPEGDA) also elicit similar cytotoxicity to those of PLLA (Fig. 9B), a biodegradable polymer widely-used in FDA approved medical devices. To demonstrate the utility of PPEGMC hydrogels as a cell delivery system, cells were seeded on the surface of PPEGMCs and encapsulated within the *in situ* forming networks of PPEGMC. Both NIH 3T3 fibroblasts and human dermal fibroblasts adhered and spread on the surface (Fig. 8). Upon encapsulation, more than 80% of NIH 3T3 cells were viable within the networks of PPEGMCs and began to spread after 48 h of encapsulation. These cell culture results clearly demonstrated the potentials of using PEGMC as an injectable cell delivery carrier.

To further demonstrate the injectability of PEGMCs for *in vivo* applications, we have demonstrated that PEGMCs could be injected into rats subcutaneously with a 27 G needle and could be crosslinked *in situ* within a few minutes (Fig. 10). The optimal amount of water-soluble redox initiators were used to allow enough time for injection before PEGMCs were crosslinked *in situ*. Histology analysis demonstrated that PPEGMCs elicited slight inflammation in the early stages post-injection (Fig. 11 and 12). Upon complete degradation of the hydrogel (30 d), the inflammatory active zone was significantly reduced with minimal cell infiltration in the implantation sites. The relatively faster degradation *in vivo* might result from enzyme degradation that would normally occur to many other types of polyesters when implanted in the body. The above animal studies clearly indicate the *in situ* formation of PPEGMC hydrogels and the excellent *in vivo* tissue compatibility and degradability.

The development of water-soluble CA-derived PEGMC injectable biomaterials opens many options for future innovations. The use of CA as a key monomer for PEGMC synthesis brings many opportunities for biomaterial innovations. As mentioned previously, the available –COOH and –OH from citrate units on the polymer backbones can be used for bioconjugation with drug/ proteins to make biofunctional injectable materials. CA has brought a benefit that a high percentage of hydroxyapatite (HA) (up to 65%, similar to the percentage of inorganic components in native bones) could be incorporated with previously developed CA-derived poly(diol citrates) due to intimate interactions of HA and the calcium-chelating citrate units of polymers.[7] The high percentage of HA incorporated into poly(diol citrates) makes poly(diol citrates)/HA a promising composite material that enables inducing rapid mineralization, reinforcing mechanical properties, and enhancing biocompatibility for bone tissue engineering applications. We are actively studying the development of injectable *in situ* forming PEGMA/HA bone tissue engineering scaffolds for large-bone defect regeneration. Also, PEGMCs can potentially be made into *in situ* injectable biodegradable photoluminescent polymers by adding α-amino acids in polymer syntheses similar to the syntheses of CA-derived BPLPs.[11] Such injectable photoluminescent polymers may open new avenues in studying *in vivo* cell/drug delivery and tissue engineering using bioimaing tools.

5. Conclusion

We reported the syntheses and characterization of a CA-derived biodegradable injectable hydrogel, PEGMC. The syntheses of PEGMC hydrogels was a convenient one-pot reaction without the use of any organic solvents or catalysts. Water-soluble PEGMC demonstrated excellent injectability, *in situ* crosslinkability, adequate functionalities, elastic mechanical properties, and controlled degradability. The crosslinked PEGMC (PPEGMC) demonstrated excellent cytocompatibility *in vitro*, minimal inflammation *in vivo*, and degradability *in vitro* and *in vivo*. Collectively, the development of the platform injectable PEGMC biomaterials adds new members of CAderived biodegradable polymers and presents unique opportunities for many biomedical applications such as bone tissue engineering and drug delivery.

Acknowledgments

This work was supported in part by a Beginning Grant-in-Aid award from the American Heart Association (AHA), an award R21EB009795 from the National Institute of Biomedical Imaging and Bioengineering (NIBIB), a seed grant from Texas Scottish Rite Hospital for Children (TSRHC), and a National Science Foundation (NSF) CAREER award 0954109.

References

1. Tran RT, Zhang Y, Gyawali D, Yang J. Recent development on citric acid derived biodegradable elastomers. Recent Pat Biomed Eng 2009;2:216–227.
2. Tran RT, Thevenot P, Zhang Y, Gyawali D, Tang L, Yang J. Scaffold sheet design strategy for soft tissue engineering. Materials 2010;2:1375–1389.
3. Yang J, Webb AR, Pickerill SJ, Hageman G, Ameer GA. Synthesis and evaluation of poly(diol citrate) biodegradable elastomers. Biomaterials 2006;27(9):1889–1898. [PubMed: 16290904]
4. Yang J, Webb AR, Hageman G, Ameer GA. Novel citric acid-based biodegradable elastomers for tissue engineering. Adv Mater 2004;16:511–516.
5. Yang J, Motlagh D, Allen JB, Webb AR, Kibbe MR, Aalami O, et al. Modulating expanded polytetrafluoroethylene vascular graft host response via citric acid-based biodegradable elastomers. Adv Mater 2006;18(12):1493–1498.
6. Yang J, Motlagh D, Webb AR, Ameer GA. Novel biphasic elastomeric scaffold for small-diameter blood vessel tissue engineering. Tissue Eng 2005;11(11–12):1876–1886. [PubMed: 16411834]
7. Qiu HJ, Yang J, Kodali P, Koh J, Ameer GA. A citric acid-based hydroxyapatite composite for orthopedic implants. Biomaterials 2006;27(34):5845–5854. [PubMed: 16919720]

8. Dey J, Xu H, Shen JH, Thevenot P, Gondi SR, Nguyen KT, et al. Development of biodegradable crosslinked urethane-doped polyester elastomers. Biomaterials 2008;29(35):4637–4649. [PubMed: 18801566]

9. Gyawali D, Tran RT, Guleserian K, Tang L, Yang J. Citric-acid-derived photo-cross-linked biodegradable elastomers. J Biomat Sci-Polym E 2010;21:1761–1782.

10. Tran RT, Thevenot P, Gyawali D, Chiao J-C, Tang L, Yang J. Development of a novel biodegradable elastomer featuring a dual crosslinking mechanism for soft tissue engineering. Soft Matter 2010;6:2449–2461.

11. Yang J, Zhang Y, Gautam S, Liu L, Dey J, Chen W, et al. Development of aliphatic biodegradable photoluminescent polymers. Proc Natl Acad Sci U S A 2009;106(25):10086–10091. [PubMed: 19506254]

12. Hennink WE, van Nostrum CF. Novel crosslinking methods to design hydrogels. Adv Drug Deliv Rev 2002;54(1):13–36. [PubMed: 11755704]

13. Payne RG, Yaszemski MJ, Yasko AW, Mikos AG. Development of an injectable, in situ crosslinkable, degradable polymeric carrier for osteogenic cell populations. Part 1. Encapsulation of marrow stromal osteoblasts in surface crosslinked gelatin microparticles. Biomaterials 2002;23(22):4359–4371. [PubMed: 12219826]

14. Stile RA, Healy KE. Thermo-responsive peptide-modified hydrogels for tissue regeneration. Biomacromolecules 2001;2(1):185–194. [PubMed: 11749171]

15. Lutolf MP, Hubbell JA. Synthesis and physicochemical characterization of end-linked poly(ethylene glycol)-co-peptide hydrogels formed by Michael-type addition. Biomacromolecules 2003;4(3):713–722. [PubMed: 12741789]

16. Temenoff JS, Mikos AG. Injectable biodegradable materials for orthopedic tissue engineering. Biomaterials 2000;21(23):2405–2412. [PubMed: 11055288]

17. Kretlow JD, Klouda L, Mikos AG. Injectable matrices and scaffolds for drug delivery in tissue engineering. Adv Drug Deliv Rev 2007;59(4–5):263–273. [PubMed: 17507111]

18. Ifkovits JL, Burdick JA. Review: Photopolymerizable and degradable biomaterials for tissue engineering applications. Tissue Eng 2007;13(10):2369–2385. [PubMed: 17658993]

19. Nguyen KT, West JL. Photopolymerizable hydrogels for tissue engineering applications. Biomaterials 2002;23(22):4307–4314. [PubMed: 12219820]

20. Qingpu Hou PADB, Kevin M Shakesheff. Injectable scaffolds for tissue regeneration. J Mater Chem 2004;14:1915–2023.

21. Hatefi A, Amsden B. Biodegradable injectable in situ forming drug delivery systems. J Control Release 2002;80(1–3):9–28. [PubMed: 11943384]

22. Shu XZ, Ahmad S, Liu YC, Prestwich GD. Synthesis and evaluation of injectable, in situ crosslinkable synthetic extracellular matrices for tissue engineering. J Biomed Mater Res A 2006;79A(4):902–912. [PubMed: 16941590]

23. Prestwich GD. In situ crosslinkable synthetic extracellular matrices for tissue engineering and repair. FASEB J 2006;20(4):A21–A21.

24. Rowley JA, Madlambayan G, Mooney DJ. Alginate hydrogels as synthetic extracellular matrix materials. Biomaterials 1999;20(1):45–53. [PubMed: 9916770]

25. Jeon O, Bouhadir KH, Mansour JM, Alsberg E. Photocrosslinked alginate hydrogels with tunable biodegradation rates and mechanical properties. Biomaterials 2009;30(14):2724–2734. [PubMed: 19201462]

26. Ono K, Ishihara M, Ozeki Y, Deguchi H, Sato M, Saito Y, et al. Experimental evaluation of photo-crosslinkable chitosan as a biologic adhesive with surgical applications. Surgery 2001;130(5):844–850. [PubMed: 11685194]

27. Ono K, Saito Y, Yura H, Ishikawa K, Kurita A, Akaike T, et al. Photo-crosslinkable chitosan as a biological adhesive. J Biomed Mater Res 2000;49(2):289–295. [PubMed: 10571917]

28. Nuttelman CR, Henry SM, Anseth KS. Synthesis and characterization of photocrosslinkable, degradable poly(vinyl alcohol)-based tissue engineering scaffolds. Biomaterials 2002;23(17):3617–3626. [PubMed: 12109687]

29. Schmedlen KH, Masters KS, West JL. Photocrosslinkable polyvinyl alcohol hydrogels that can be modified with cell adhesion peptides for use in tissue engineering. Biomaterials 2002;23(22):4325–4332. [PubMed: 12219822]
30. Sawhney AS, Pathak CP, van Rensburg JJ, Dunn RC, Hubbell JA. Optimization of photopolymerized bioerodible hydrogel properties for adhesion prevention. J Biomed Mater Res 1994;28(7):831–838. [PubMed: 8083251]
31. Scott RA, Peppas NA. Highly crosslinked, PEG-containing copolymers for sustained solute delivery. Biomaterials 1999;20(15):1371–1380. [PubMed: 10454008]
32. Fisher JP, Tirnmer MD, Holland TA, Dean D, Engel PS, Mikos AG. Photoinitiated cross-linking of the biodegradable polyester poly(propylene fumarate). Part I. Determination of network structure. Biomacromolecules 2003;4(5):1327–1334. [PubMed: 12959602]
33. Fisher JP, Holland TA, Dean D, Engel PS, Mikos AG. Synthesis and properties of photocross-linked poly(propylene fumarate) scaffolds. J Biomat Sci-Polym E 2001;12(6):673–687.
34. Wang DA, Williams CG, Li QA, Sharma B, Elisseeff JH. Synthesis and characterization of a novel degradable phosphate-containing hydrogel. Biomaterials 2003;24(22):3969–3980. [PubMed: 12834592]
35. Ding TLQ, Shi R, Tian M, Yang J, Zhang LQ. Synthesis, characterization and in vitro degradation study of a novel and rapidly degradable elastomer. Polym Degrad Stab 2006;91:733–739.
36. Mizutani M, Matsuda T. Photocurable liquid biodegradable copolymers: In vitro hydrolytic degradation behaviors of photocured films of coumarin-endcapped poly(epsilon-caprolactone-co-trimethylene carbonate). Biomacromolecules 2002;3(2):249–255. [PubMed: 11888308]
37. Burdick JA, Padera RF, Huang JV, Anseth KS. An investigation of the cytotoxicity and histocompatibility of in situ forming lactic acid based orthopedic biomaterials. J Biomed Mater Res 2002;63(5):484–491. [PubMed: 12209891]
38. Gunatillake PA, Adhikari R. Biodegradable synthetic polymers for tissue engineering. Eur Cell Mater 2003;5:1–16. discussion 16. [PubMed: 14562275]
39. Webb AR, Yang J, Ameer GA. Novel elastomers for cardiovascular tissue engineering. Abstracts of Papers of the American Chemical Society 2004;227:U242–U42.
40. Amoa K. Catalytic Hydrogenation of Maleic Acid at Moderate Pressures: A Laboratory Demonstration. J Chemical Educ 2007;84:1948.
41. Daruwalla J, Greish K, Malcontenti-Wilson C, Muralidharan V, Iyer A, Maeda H, et al. Styrene maleic acid-pirarubicin disrupts tumor microcirculation and enhances the permeability of colorectal liver metastases. J Vasc Res 2008;46(3):218–228. [PubMed: 18953175]
42. Bettinger CJ, Bruggeman JP, Borenstein JT, Langer RS. Amino alcohol-based degradable poly(ester amide) elastomers. Biomaterials 2008;29(15):2315–2325. [PubMed: 18295329]
43. Wong TW, Wahab S, Anthony Y. Drug release responses of zinc ion crosslinked poly(methyl vinyl ether-co-maleic acid) matrix towards microwave. Int J Pharm 2008;357(1–2):154–163. [PubMed: 18329203]
44. Bruggeman JP, Bettinger CJ, Nijst CLE, Kohane DS, Langer R. Biodegradable xylitol-based polymers. Adv Mater 2008;20(10):1922–1927.
45. Poon YF, Cao Y, Zhu Y, Judeh ZM, Chan-Park MB. Addition of beta-malic acid-containing poly (ethylene glycol) dimethacrylate to form biodegradable and biocompatible hydrogels. Biomacromolecules 2009;10(8):2043–2052. [PubMed: 19603795]

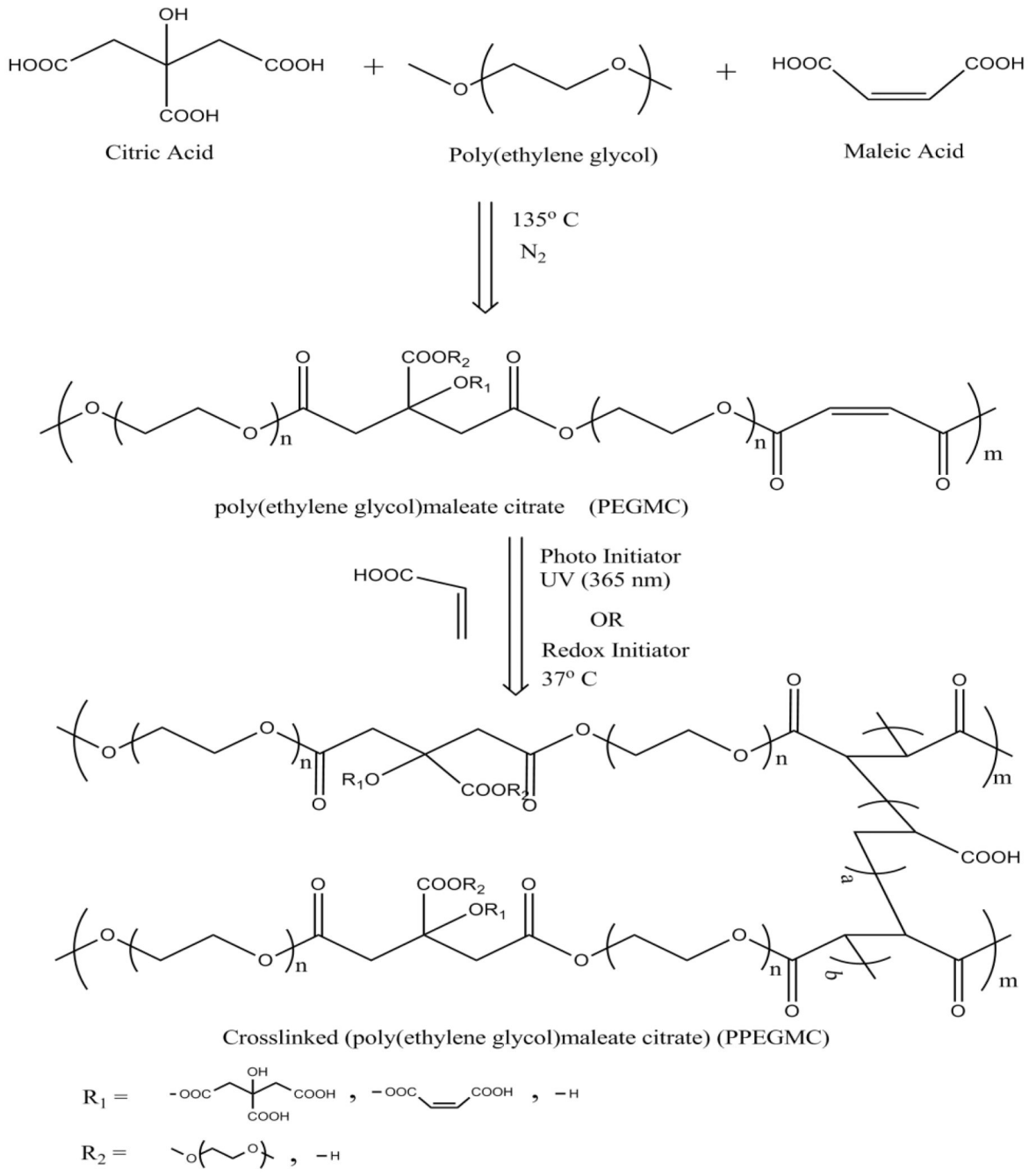

Figure 1. Schematic representation of PPEGMC synthesis

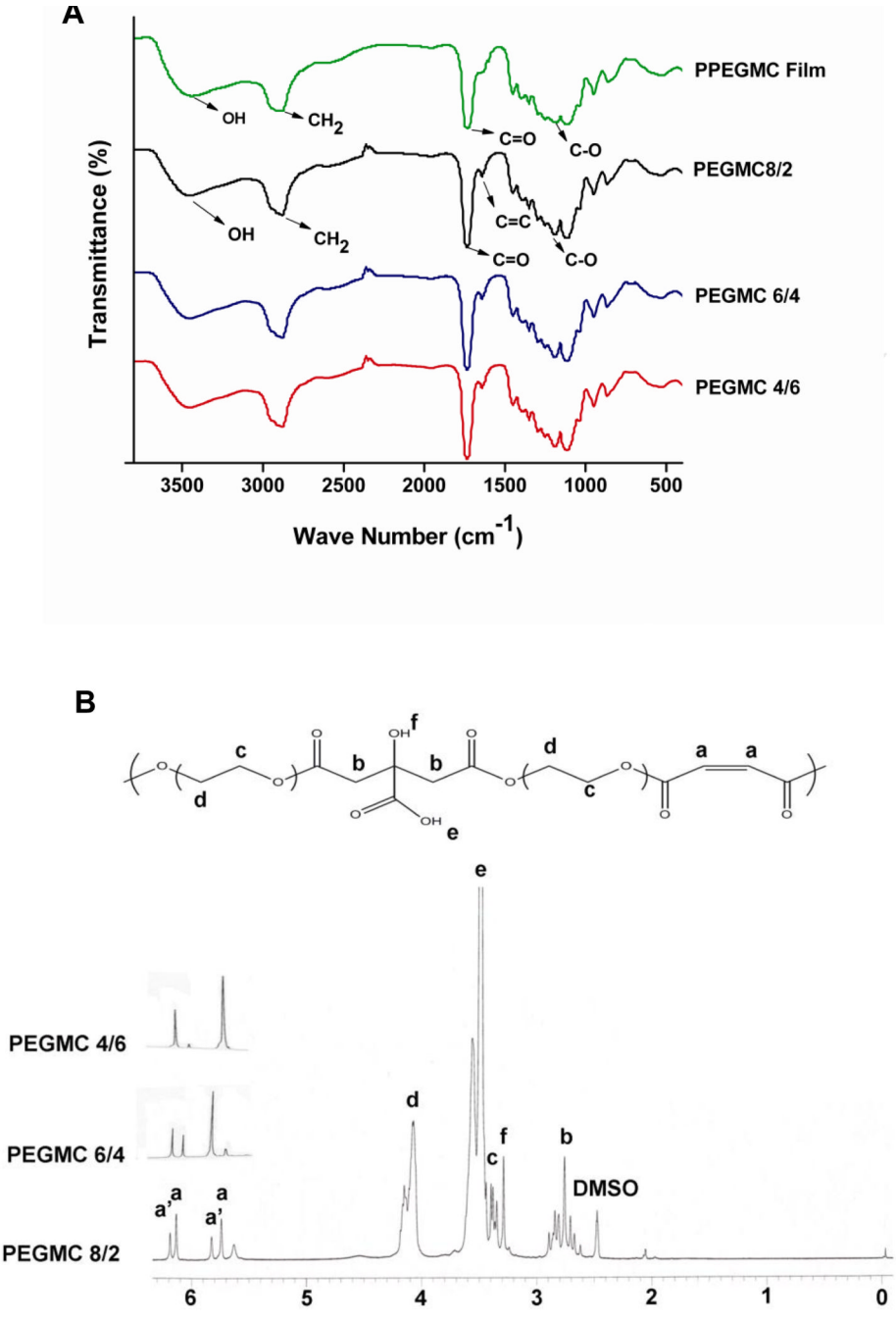

Figure 2. Polymer Characterization of PEGMC

A) FTIR spectra of the PEGMC and the photocrosslinked PPEGMC; B) ^{1}H NMR spectrum of a representative PEGMC, PEGMC8/2.

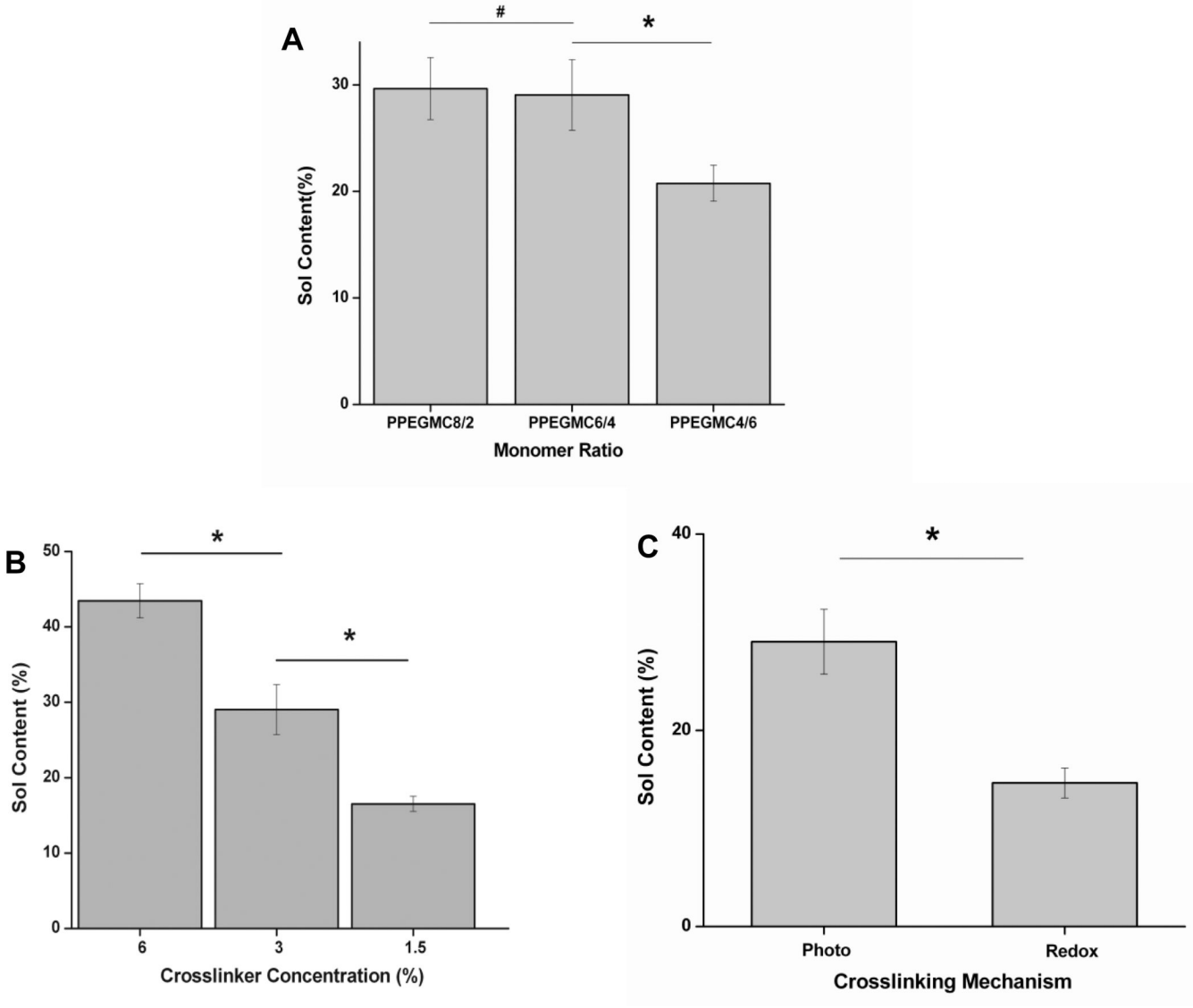

Figure 3. Sol content of PPEGMC

A) Sol content of the PPEGMC8/2, PPEGMC6/4, and PPEGMC4/6 crosslinked with 3 v/v% of crosslinker and 0.11 M of photoinitiator for 1 min. under UV radiation; B) Sol content of the PPEGMC6/4 crosslinked with 1.5 v/v%, 3 v/v%, and 6 v/v% of crosslinker and 0.11 M of photoinitiator for 1 min under UV radiation; C) Sol content of the PPEGMC6/4 initiated by photoinitiators and redox initiators. (*$p < 0.01$, $^{\#}p>0.01$).

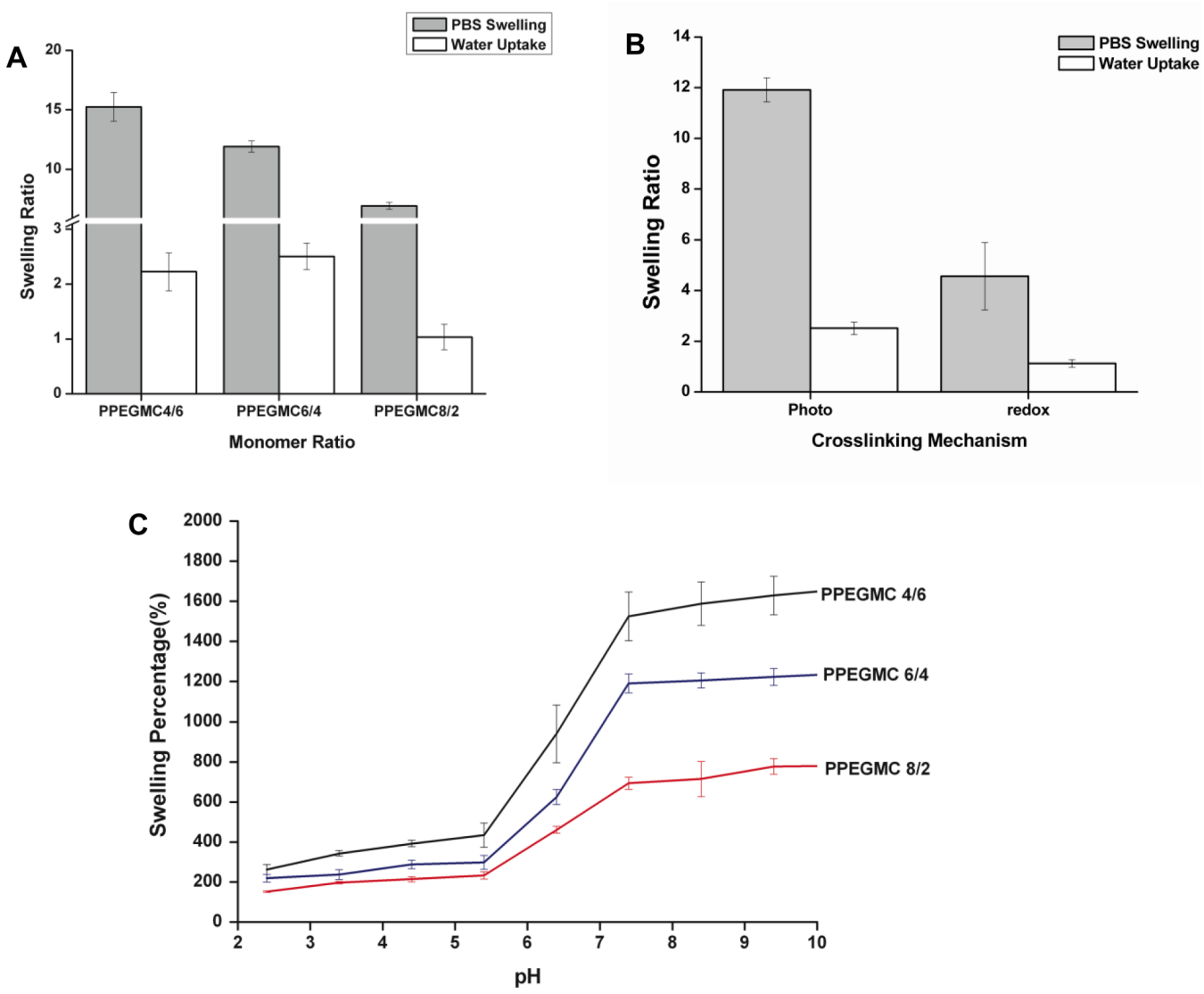

Figure 4. Swelling characterization of PPEGMC

A) Swelling ratios of the photocrosslinked PPEGMC8/2, PPEGMC6/4, and PPEGMC4/6 crosslinked with 3 v/v% of crosslinker and 0.11 M of photoinitiator for 1 min under UV radiation; B) Swelling ratios of the PPEGMC 6/4 in water and PBS at 37° C; C) Swelling ratios of the PPEGMC 6/4 crosslinked with 3 v/v% of crosslinker and 0.11 M of photoinitiator for 1 min under UV radiation in buffer solutions at different pH.

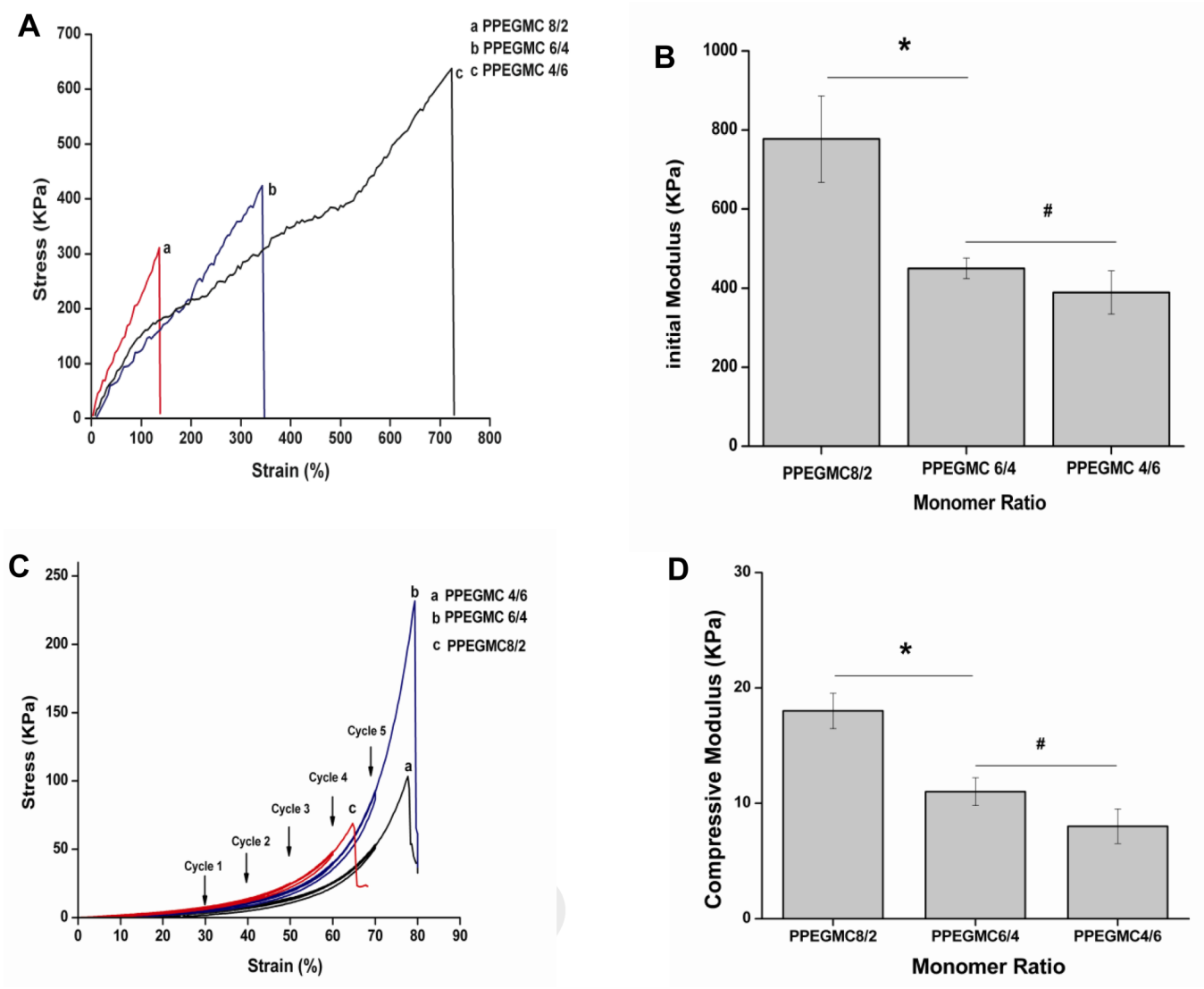

Figure 5. Mechanical Properties of PPEGMC

A) Tensile stress-strain curve, B) initial modulus, and C) cyclic compressive stress-strain curve of the photocrosslinked PPEGMC8/2, PPEGMC6/4, and PPEGMC4/6; All the above PPEGMCs were crosslinked with 3 v/v% of crosslinker and 0.11 M of photoinitiator for 1 min under UV radiation; D) Initial modulus of the hydrated redox crosslinked PPEGMC8/2, PPEGMC6/4, and PPEGMC4/6 under the cyclic compressive tests. PPEGMCs were crosslinked with 3 v/v% of crosslinker, 0.026 M of APS and 0.11 M of TEMED for 1 min at 37° C. (*$p < 0.01$, #$p>0.01$).

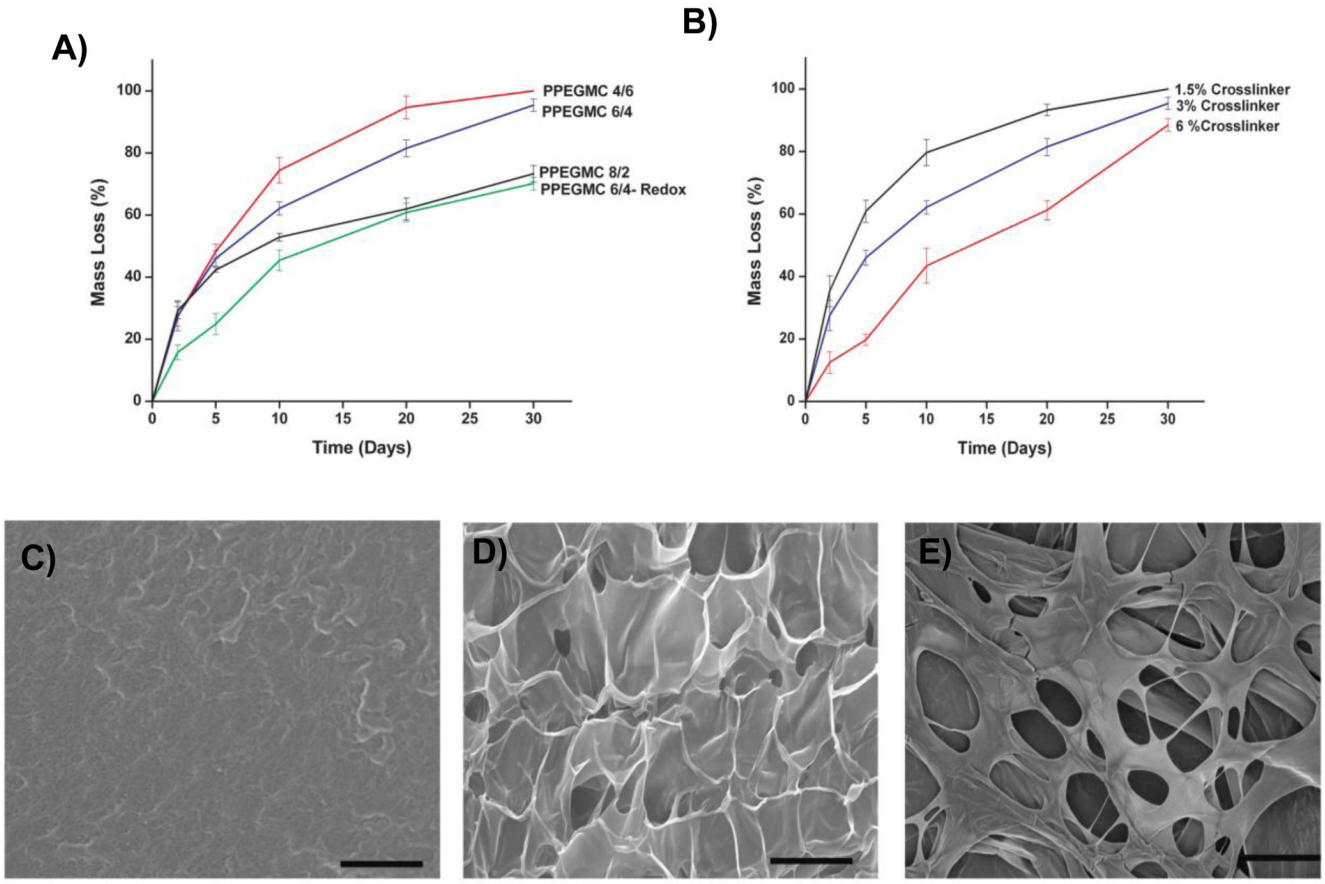

Figure 6. ***In vitro*** **degradation of PPEGMC**

A) Mass loss of the photocrosslinked PPEGMCs and redox crosslinked (PPEGMC-Redox) hydrogels incubated in PBS (pH 7.4; 37° C) for up to 1 30 days; B) Mass loss of the photocrosslinked PPEGMC 6/4 crosslinked with 1.5, 3, and 6 v/v% of crosslinkers; SEM image of the degrading PPEGMC6/4 film at C) day 5, D) day 10, and E) day 20. PPEGMC exhibited smooth surface at day 5 and gradually turn into porous matrix over time. All scale bar = 200 μm.

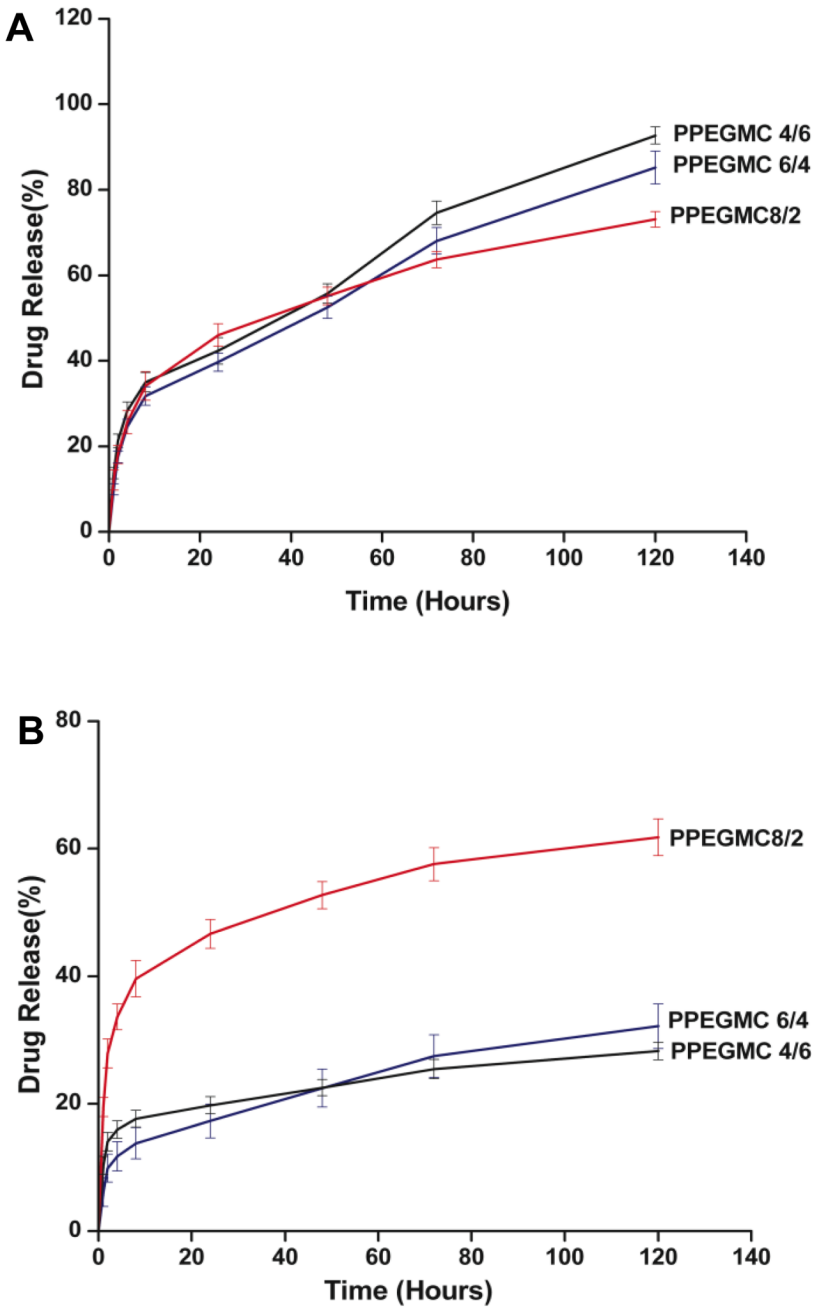

Figure 7. Cumulative release of BSA from photo-crosslinked PPEGMC hydrogels at 37° C
A) Release profile of BSA from PBS solutions (pH = 7.4). B) Release profile of BSA from sodium acetate-acetic acid buffer solution (pH = 5.4).

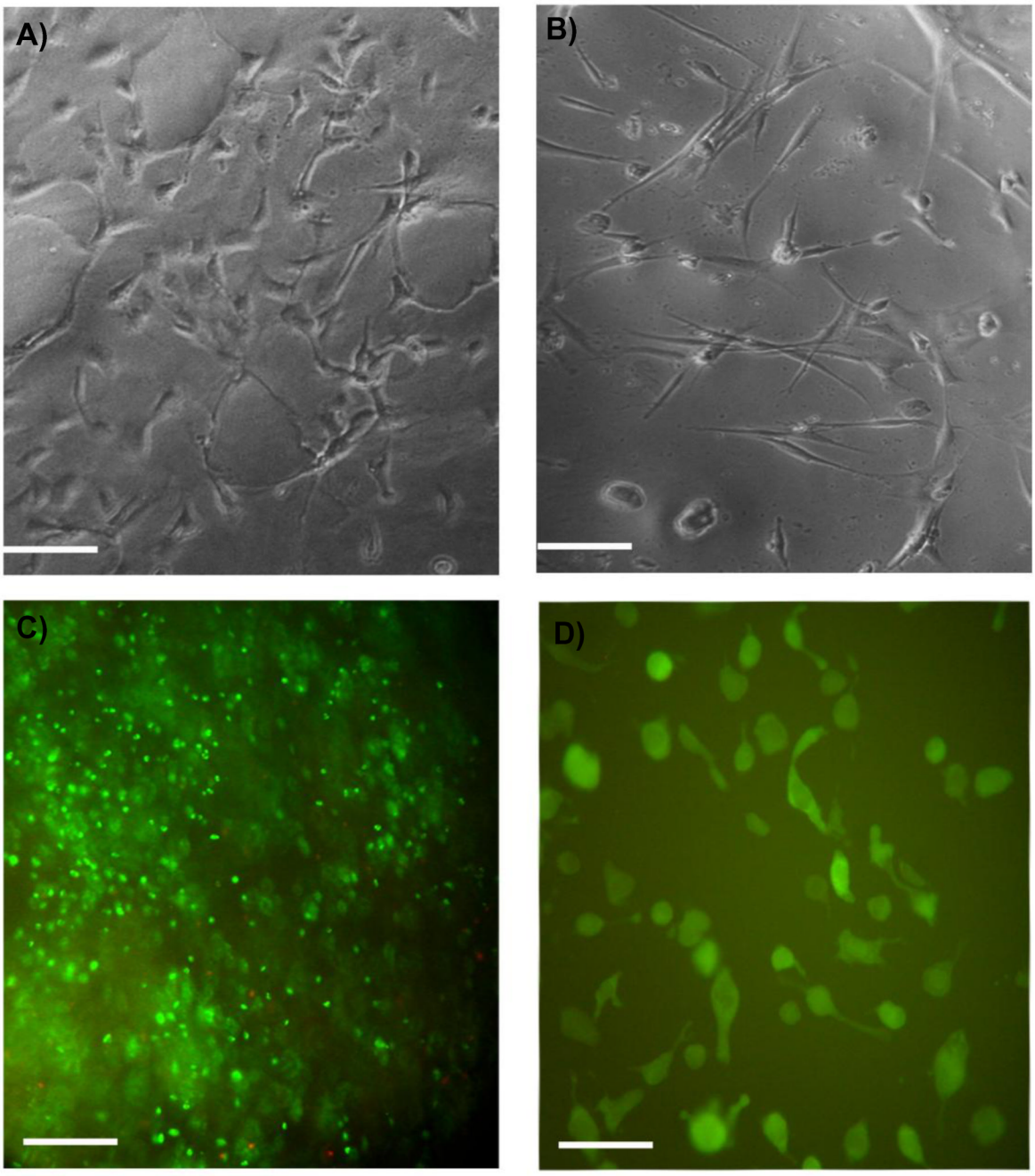

Figure 8. NIH 3T3 fibroblasts culture on or within PPEGMC hydrogels

Representative photomicrograph of A) NIH 3T3 fibroblasts and B) human dermal fibroblasts adhered and spread on photocrosslinked PPEGMC 6/4 hydrogel surface 48 hours after initial seeding; C) Live (green stain)-Dead (red stain) assay of NIH 3T3 fibroblasts encapsulated within the network of redox crosslinked PPEGMC 6/4 48 hours after seeding; D) CFDA-SE labeled NIH 3T3 fibroblasts spread within the network of RPPEGMC 6/4 48 hours after seeding (scale bar 200 μm).

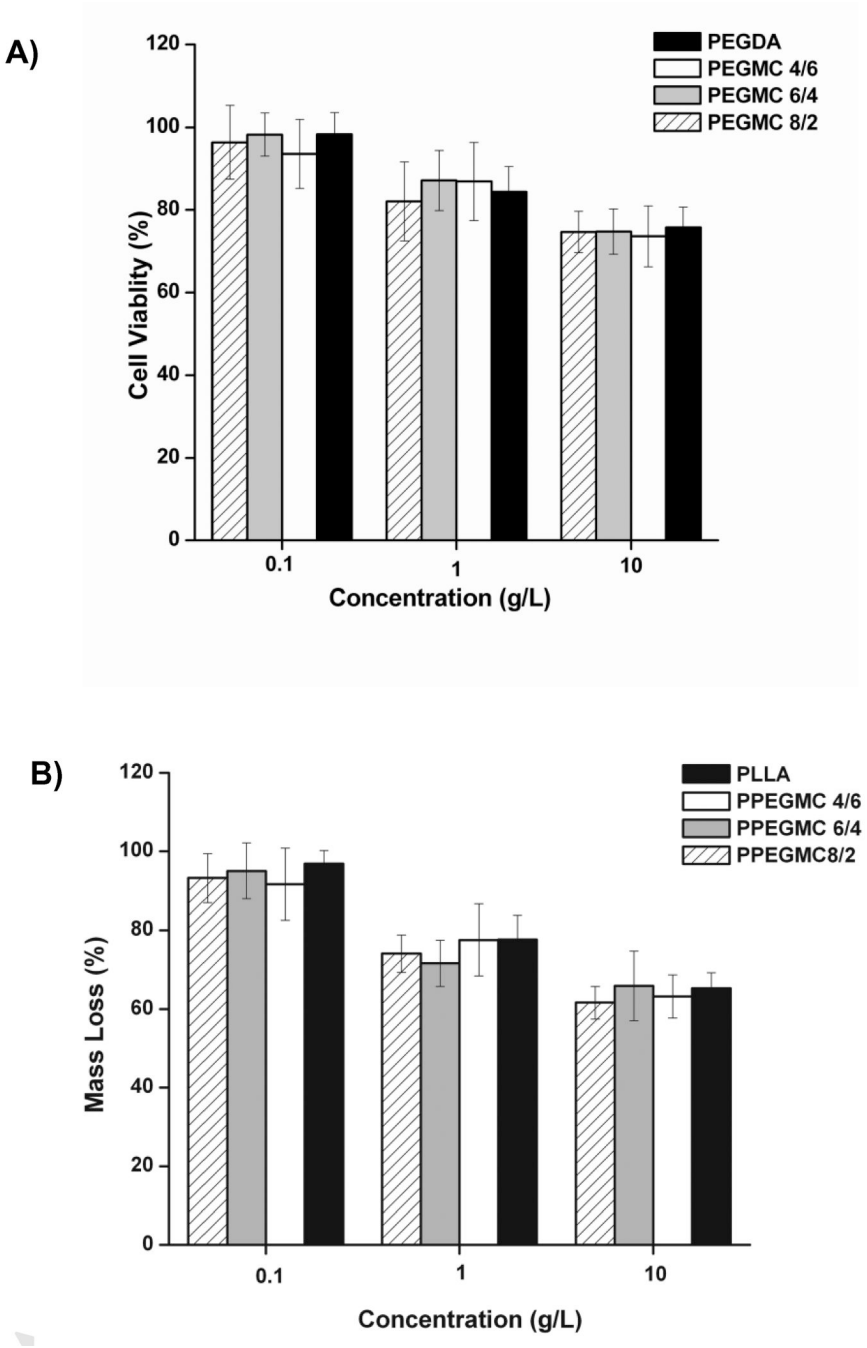

Figure 9. Cytotoxicity evaluation

of A) water-soluble PEGMCs and B) the degradation products of PPEGMC hydrogels via MTT assay. PEGDA was used as a control for PEGMCs. PLA was used as a control for PPEGMCs.

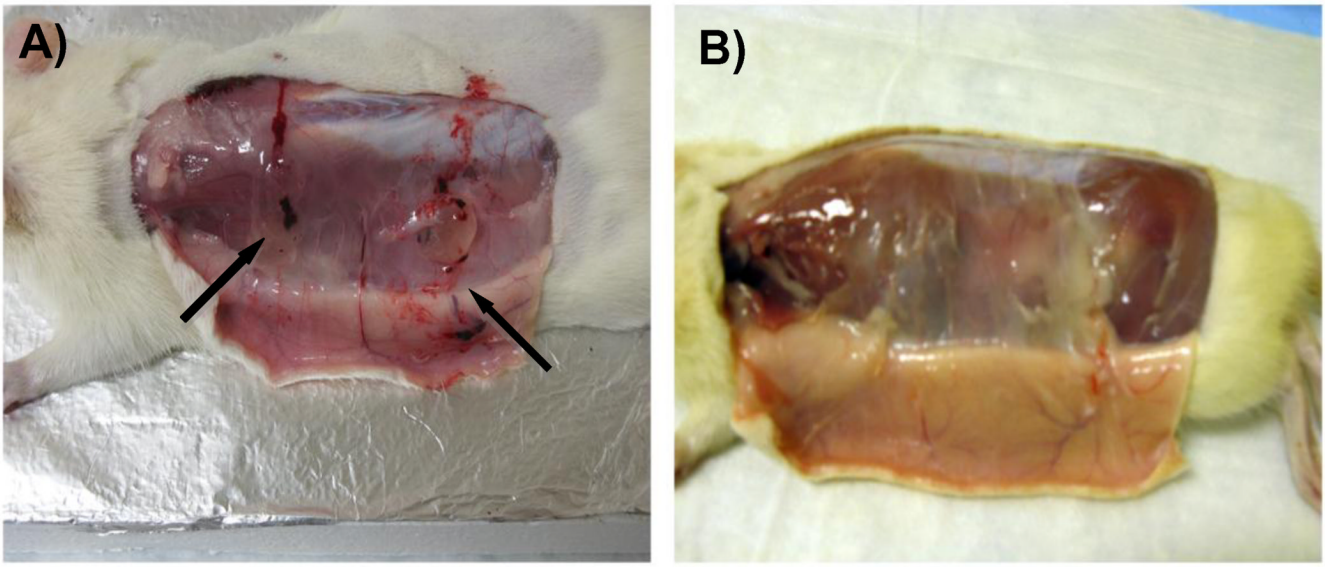

Figure 10. In-situ crosslinkability and in vivo degradation of PPEGMC hydrogels

A) PEGMC crosslinking into PPEGMC hydrogel in 3 minutes after injection subcutaneously in a Sprague-Dawley rat through a 27-gauge needle; B) In-situ formed PPEGMC hydrogel completely degraded/absorbed within 30 days in vivo.

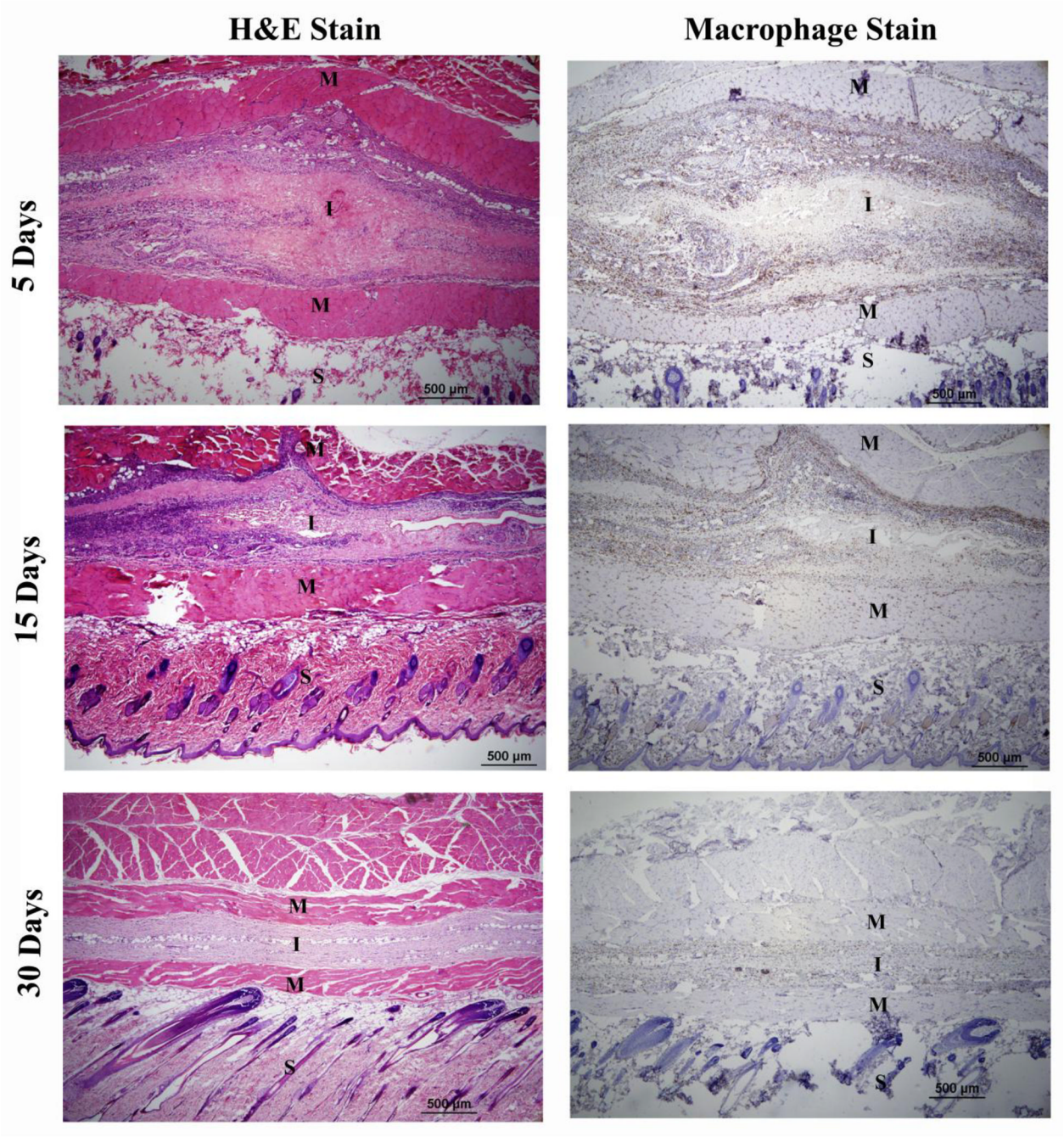

Figure 11. Host responses to PPEGMC implanted subcutaneously in Sprague-Dawley rats

Histology (H&E staining and macrophage staining (CD68+) analysis demonstrated that PPEGMC elicited slight inflammation in the early stages post-injection (day 5 and 15). Upon complete degradation of the hydrogel (day 30), the inflammatory active zone was significantly reduced with minimal cell infiltration in the implantation sites. S, M, and I represent skin, muscle, and implantation site respectively.

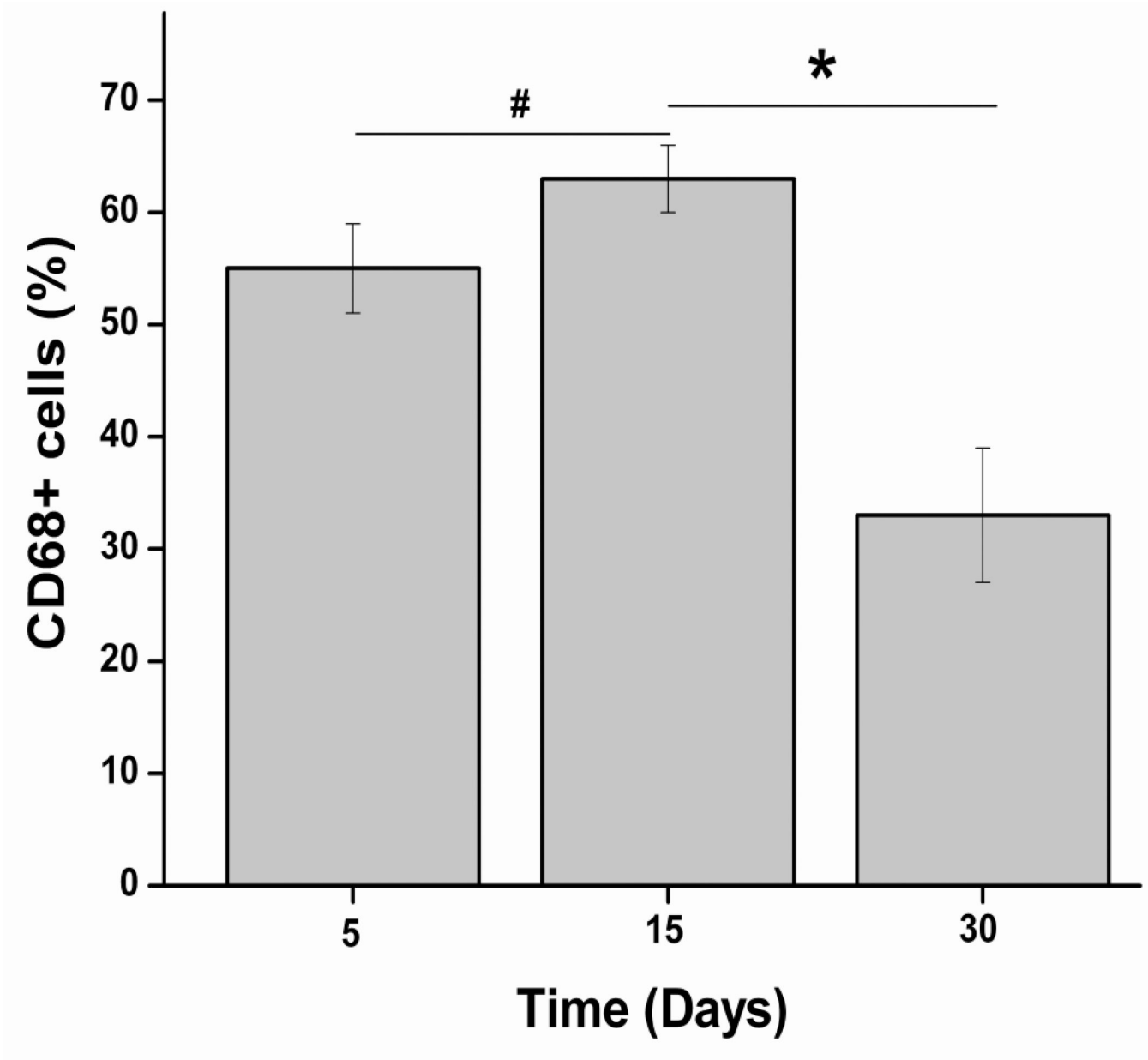

Figure 12.
Quantification of the percentage of macrophages (stained as CD68+ cells) presence in the inflammatory active zone (*$p < 0.01$, $^{\#}p>0.01$). The number of CD68 positive cells did not significantly increase with increasing implant duration from day 5 to day 15. However, the number of macrophages was significantly decreased as the material gradually absorbed by the host at day 30.

Table 1

Feeding ratios and actual compositions of PEGMC. Actual compositions of the polymer were calculated by integrating the area of characteristic peaks illustrated in ^{1}H-NMR spectra.

Polymer Name	MA:CA:OD (moles)	Feeding Ratio MA:CA:OD	Composition MA:CA:OD
PPEGMC 8/2	0.08/0.02/0.10	0.4/0.1/0.50	0.37/0.12/0.50
PPEGMC 6/4	0.06/0.04/0.10	0.3/0.2/0.50	0.28/0.20/0.52
PPEGMC 4/6	0.04/0.06/0.10	0.2/0.3/0.50	0.17/0.31/0.48